We are IntechOpen,
the world's leading publisher of Open Access books
Built by scientists, for scientists

6,900
Open access books available

185,000
International authors and editors

200M
Downloads

154
Countries delivered to

Our authors are among the

TOP 1%
most cited scientists

12.2%
Contributors from top 500 universities

CLARIVATE ANALYTICS
BOOK CITATION INDEX
INDEXED

WEB OF SCIENCE™

Selection of our books indexed in the Book Citation Index
in Web of Science™ Core Collection (BKCI)

Interested in publishing with us?
Contact book.department@intechopen.com

Numbers displayed above are based on latest data collected.
For more information visit www.intechopen.com

All-Ceramic Percolative Composites with a Colossal Dielectric Response

Vid Bobnar, Marko Hrovat, Janez Holc and Marija Kosec
Jožef Stefan Institute, Jamova 39, SI-1000, Ljubljana
Slovenia

1. Introduction

Dielectric materials, which are used to control and store charges and electric energy, play a key role in modern electronics and electric power systems. As commercial and consumer requirements for compact and low cost electronic and electrical power systems as well as for very high energy capacitive storage systems grow substantially, the development of high dielectric constant materials has become one of the major scientific and technology issues (Reynolds & Buchanan, 2004; Scott, 2007). High dielectric constant materials are highly desirable for use, not only as capacitor dielectrics, but also in a broad range of advanced electromechanical applications, such as actuators, sonars, and, particularly, as high-frequency transducers (Zhang et al., 2002). The input electric energy that can be converted into the strain energy is namely directly proportional to the square of the electric field and to the dielectric constant of the electroactive material. Thus, by increasing the dielectric constant the required electromechanical response, i.e., strain can be induced under a much reduced electric field.

Extremely large dielectric constants are expected only for ferroelectrics in a very narrow temperature range close to the paraelectric-to-ferroelectric phase transition or for systems with hopping charge carriers yielding dielectric constant that diverges towards low frequencies. High-capacitance ceramic capacitors are therefore mostly made of very thin layers of ceramic material (usually a ferroelectric) placed between conductive plates. The most important part of the market in passive devices is, at present, made up of multilayer ceramic capacitors (MLCCs), comprising alternating thin layers of conductor (inner electrodes) and ceramic (Takeshima et al., 1997), which turns out to be the most efficient geometry for attaining high-density charge storage. A similar geometrical approach can also intuitively explain the dielectric response of a percolative composite – a composite comprising a conductive filler embedded in a dielectric matrix. The fact that the effective dielectric constant of the mixture is much larger than the dielectric constants of the individual constituents is due to the fact that close to the percolation point (the volume fraction when the conductive admixture forms a continuous network and, consequently, the system begins to conduct electricity) there are many conducting particles which are isolated by very thin dielectric/ferroelectric layers. A comparison between configurations of a MLCC and a percolative composite is presented in Fig. 1. Unfortunately, the percolative

approach in developing high dielectric constant materials has up to now very often been handicapped by the impossibility of preparing homogeneous metal–insulator composites with metal concentrations very close to the percolation threshold.
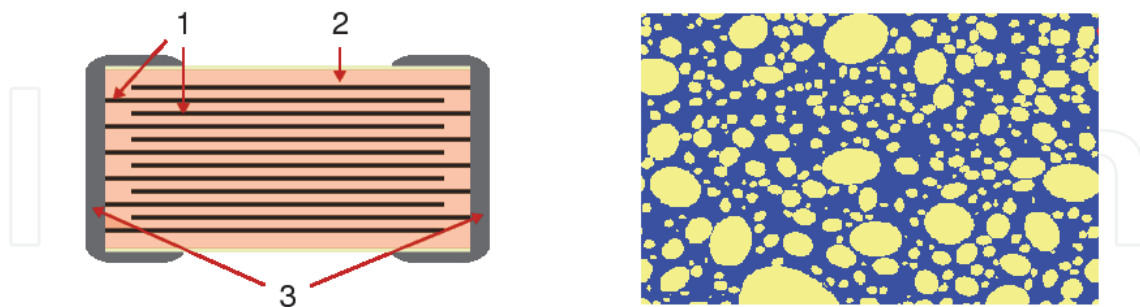

Fig. 1. Schematic configuration of a multilayer ceramic capacitor (MLCC) (left; 1-metallic electrodes, 2-thin layers of dielectric/ferroelectric ceramics, 3-metallic contacts) and a percolative composite (right; yellow and blue regions represent conductive and dielectric/ferroelectric material, respectively).

Exceptionally high dielectric constants which were obtained by making use of the conductive percolative phenomenon in ceramic composites made of perovskite ruthenium-based conductive ceramics and perovskite ferroelectric ceramics, are reported in this chapter. The potential of these all-ceramic percolative composites for use as high dielectric constant materials in various applications is demonstrated: Due to a homogeneous distribution of conductive ceramic grains within the ferroelectric ceramic matrix, the dielectric response of the lead-based $Pb(Zr,Ti)O_3$–$Pb_2Ru_2O_{6.5}$ and $0.65Pb(Mg_{1/3}Nb_{2/3})O_3$-$0.35PbTiO_3$–$Pb_2Ru_2O_{6.5}$ as well as of the lead-free $(K,Na)NbO_3$–RuO_2 systems namely follows the predictions of the percolation theory. Thus, values of the dielectric constant are near the percolation threshold for two orders of magnitude higher than in the pure matrix ferroelectric ceramics.

2. Percolative composites

The theory of percolation was initially developed to describe several abrupt transitions commonly found in transport phenomena. Based on this model, a general theory was built that explains a physical process in which a macroscopic magnitude is strongly modified as a result of small microscopic changes in connectivity (Feng et al., 1987). One such process is the anomalous behavior of a metal-insulator composite near its percolation threshold, which is characterized by an abrupt discontinuity in the real part of the electrical conductivity (Bergman & Imry, 1977; Kirkpatrick, 1973). An excellent review for the system consisting of randomly distributed metallic and dielectric regions is given in the paper of Efros and Shklovskii (Efros & Shklovskii, 1976): It is shown that the static dielectric constant diverges at the percolation threshold – at the volume fraction of metallic regions (p) where the insulator-to-metal transition occurs, i.e., the static effective electrical conductivity σ of such a heterogeneous system undergoes a transition from

$$\sigma = \sigma_{matrix} \left[(p_c - p)/p_c \right]^{-q} , \tag{1}$$

which is valid below the percolation threshold p_c, into

$$\sigma = \sigma_{metal} \left[(p-p_c)/p_c \right]^t ,\qquad\qquad (2)$$

which holds true for $p>p_c$. σ_{matrix} and σ_{metal} are conductivities of the dielectric and metallic phases, respectively (of course $h=\sigma_{matrix}/\sigma_{metal}<<1$). This behavior is depicted in Fig. 2, which also reveals that a smooth transition from Eq. (1) to Eq. (2) occurs in some small interval Δ near the percolation point.
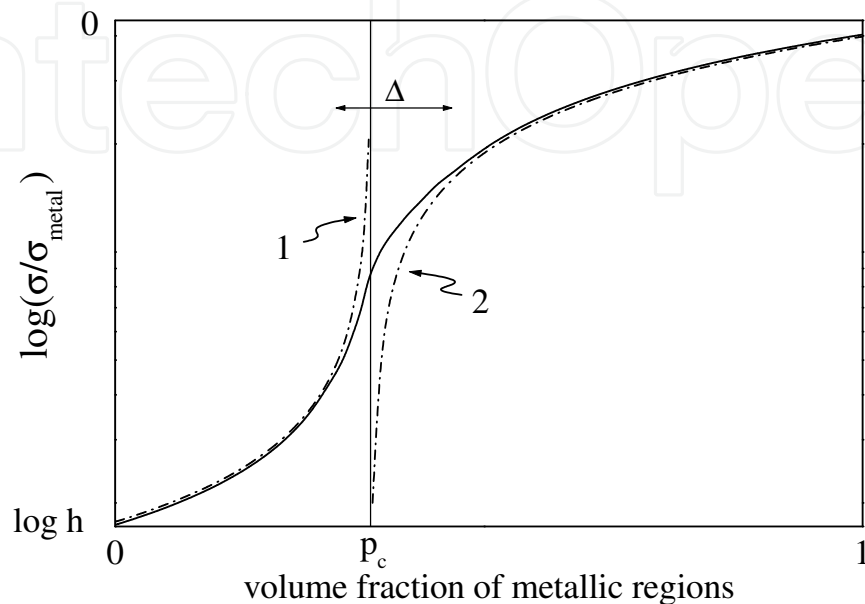

Fig. 2. The theoretical dependence of the effective electrical conductivity σ (solid line) for a system consisting of randomly distributed metallic and dielectric regions. A smooth transition between behaviors described by Eqs. (1) and (2) (dash-dotted lines) occurs in small interval Δ near the percolation point p_c (vertical line).

Very high dielectric constants can thus be achieved in metal-insulator composites close to the percolation point. However, up to now mainly organic percolative composites (Dang et al., 2003; Huang et al., 2004; Xu & Wong, 2005) and inorganic composites comprising metal particles dispersed in a dielectric matrix (Deepa et al., 2007; Grannan et al., 1981; Li et al., 2001; Yoshida, 1990) have been developed. In organic percolative composites values of the dielectric constant as high as 7000 were obtained (Huang & Zhang, 2004). As the dielectric constant of a polymer is typically less than 100, i.e., far below the values of inorganic ferroelectrics, which reach several thousands, it is not surprising that the dielectric constant in percolative composites with an inorganic matrix can reach values as high as 80000 (Pecharroman et al., 2001).

2.1 All-ceramic percolative composites

Composites of ferroelectric ceramics and conductive ceramic particles can offer a major advantage in the development of high dielectric constant materials, as percolative systems comprising ceramics and metal particles are relatively sensitive to processing. The latter can be sintered in air only if a noble metal is used; however, if the conductive component is based on a non-noble metal, the system has to be fired in a neutral or reducing atmosphere. Such a procedure can negatively influence the electrical properties of ferroelectric ceramics, which are, due to the relatively high dielectric constant, very suitable for the matrix in a

percolative system. For example, insulating ferroelectric $BaTiO_3$ or $Pb(Zr,Ti)O_3$ systems can become semiconducting as a result of reduction (Raymond & Smyth, 1996). The combination of insulating and conducting ceramics is thus inherently better than the combination of oxide ceramics and metallic particles, as the all-oxide ceramic systems can be sintered in air. On the other hand, all-ceramic systems could suffer from reactions between both constituents during high-temperature sintering, resulting in new compounds or solid solutions with undesirable characteristics. The compatibility between the chosen ceramic matrix and the conductive ceramics must therefore be carefully evaluated.

3. Processing and structural analysis

3.1 Synthesis of all-ceramic percolative composites
3.1.1 $Pb(Zr,Ti)O_3$–$Pb_2Ru_2O_{6.5}$ system

$Pb(Zr,Ti)O_3$–$Pb_2Ru_2O_{6.5}$ all-ceramic percolative system was made from $PbZr_{0.53}Ti_{0.47}O_3$ (PZT) and $Pb_2Ru_2O_{6.5}$ powders. These two systems have been chosen as $Pb_2Ru_2O_{6.5}$ is a very good electrical conductor, having the resistivity of 270×10^{-8} Ωm (Pierce et al., 1982), and as investigations of the phase equilibrium in the Pb–Zr–Ti–Ru–O system showed that PZT is compatible with $Pb_2Ru_2O_{6.5}$ at least up to 1000°C (Hrovat et al., 2001). PZT powder with a 6 mol.% excess of PbO was prepared by mechanochemical synthesis (Kuščer et al., 2006) from high-purity PbO, ZrO_2, and TiO_2. The excess lead oxide was added to compensate for its evaporation during the synthesis. $Pb_2Ru_2O_{6.5}$ powder was prepared by solid-state synthesis from PbO and RuO_2 by repeated firing with intermediate grinding (three times) at 850°C. Prereacted PZT and $Pb_2Ru_2O_{6.5}$ powders were mixed, pressed into pellets and fired on platinum foils at 850°C for 15 min.

3.1.2 $0.65Pb(Mg_{1/3}Nb_{2/3})O_3$-$0.35PbTiO_3$–$Pb_2Ru_2O_{6.5}$ system

Although values of the dielectric constant as high as 40000 were detected in the PZT-$Pb_2Ru_2O_{6.5}$ composite (Bobnar et al., 2008), a further challenge was to find another ceramic system, with much higher dielectric constant as those of PZT if possible, which would also be compatible with the $Pb_2Ru_2O_{6.5}$ system. $0.65Pb(Mg_{1/3}Nb_{2/3})O_3$-$0.35PbTiO_3$ (PMN-35PT) perovskite ferroelectric, which has a very high dielectric constant as this composition is close to the morphotropic phase boundary (Priya et al., 2002), was found to be such a system, and, consequently, in the developed PMN-35PT–$Pb_2Ru_2O_{6.5}$ composite values of the dielectric constant higher than 10^5 were detected (Bobnar et al., 2009a). Similarly to the PZT, PMN-35PT powder was prepared by mechanochemical synthesis (Kuščer et al., 2007). A mixture of PbO, MgO, TiO_2, and Nb_2O_5 in the molar ratio corresponding to the stoichiometry of 0.65PMN–0.35PT with 2 mol % of the PbO excess was high-energy milled in a planetary mill for 64 hours. A total of 200 g of powder was placed in the vial. Finally, prereacted PMN-35PT and $Pb_2Ru_2O_{6.5}$ powders were mixed, pressed into pellets and fired on platinum foils at 1000°C for 4 hours.

3.1.3 Lead-free $K_{0.5}Na_{0.5}NbO_3$–RuO_2 composite

As lead represents a possible ecological hazard, a great deal of current materials research is oriented toward environmentally friendly lead-free materials. Thus, $K_{0.5}Na_{0.5}NbO_3$–RuO_2 (KNN-RuO_2) lead-free percolative composite has also been developed (Bobnar et al., 2009b): RuO_2 is a very good electrical conductor with the resistivity of 40×10^{-8} Ωm (van Loan, 1972)

and it has been found that there is no reaction between KNN and RuO_2 at temperatures even higher than 1000°C. $K_{0.5}Na_{0.5}NbO_3$ powder was prepared by solid-state synthesis from K_2CO_3, Na_2CO_3, and Nb_2O_5. A total of 2 wt.% of potassium-sodium germanate was added to lower the sintering-temperature of KNN. The powder mixtures were homogenized, calcined at 900°C for 4 hours and milled to yield submicron-sized powders. KNN and RuO_2 powders were then mixed in acetone in a ball mill. The powders were pressed into pellets and fired on platinum foils at 1000°C for 2 hours.

3.2 Characterization methods

The phase composition of the PZT, PMN-35PT, KNN, and $Pb_2Ru_2O_{6.5}$ powders was checked by X-ray powder diffraction using a Philips PW 1710 X-ray diffractometer with Cu Kα radiation. The X-ray spectra were measured from 2Θ=20° to 2Θ=70°.

Fired PZT–$Pb_2Ru_2O_{6.5}$, PMN-35PT–$Pb_2Ru_2O_{6.5}$, and KNN–RuO_2 samples were characterized using X-ray powder diffraction. A JEOL 5800 scanning electron microscope (SEM) equipped with a link ISIS 300 energy-dispersive X-ray analyzer (EDS) was used for the overall microstructural and compositional analyses. The samples prepared for the SEM were mounted in epoxy in a cross-sectional orientation and then polished using standard metallographic techniques. Prior to analysis in the SEM, the samples were coated with carbon to provide electrical conductivity and avoid charging effects. The microstructures of the polished samples were studied using back-scattered electron imaging and compositional contrast to distinguish between the phases that differ in density (average atomic number Z).

3.3 Structural properties

Microstructures and X-ray spectra of developed all-ceramic percolative composites are shown in Fig. 3. The microstructure of the PZT–$Pb_2Ru_2O_{6.5}$ composite with 15 vol.% of $Pb_2Ru_2O_{6.5}$ consists of small, light-grey inclusions ($Pb_2Ru_2O_{6.5}$) in a dark-grey matrix (sintered PZT). The small black spots are pores. PMN-35PT–$Pb_2Ru_2O_{6.5}$ microstructure (also the sample with 15 vol. % of $Pb_2Ru_2O_{6.5}$) consists of small, light-grey $Pb_2Ru_2O_{6.5}$ inclusions, a dark-grey PMN-PT matrix, and a few pores. The microstructure of the lead-free KNN–RuO_2 sample with 15 vol.% of RuO_2 reveals that the grey KNN matrix consists of cubic-shaped grains, while the light-grey inclusions are RuO_2 grains.

In each of the three composites the conductive filler is uniformly distributed throughout the matrix. The EDS microanalysis did not detect any solid solubility in developed composites, which confirms the results obtained with X-ray analyses: Only the peaks of the initial compounds are present in the fired samples and, furthermore, no shifts in the peaks' positions were observed (for comparison, the X-ray spectra of individual PZT, KNN, and $Pb_2Ru_2O_{6.5}$ constituents are included in Fig. 3). The results therefore indicate that (i) PZT and $Pb_2Ru_2O_{6.5}$, (ii) PMN-35PT and $Pb_2Ru_2O_{6.5}$, as well as (iii) KNN and RuO_2 are compatible at the firing temperatures.

Structural analysis thus revealed a demanded structure of composites – there is no reaction and no solid solubility between constituents and the conductive filler is uniformly distributed throughout the matrix. Consequently, the dielectric response of the developed PZT–$Pb_2Ru_2O_{6.5}$, PMN-35PT–$Pb_2Ru_2O_{6.5}$, and KNN-RuO_2 composites should follow the predictions of the percolation theory.
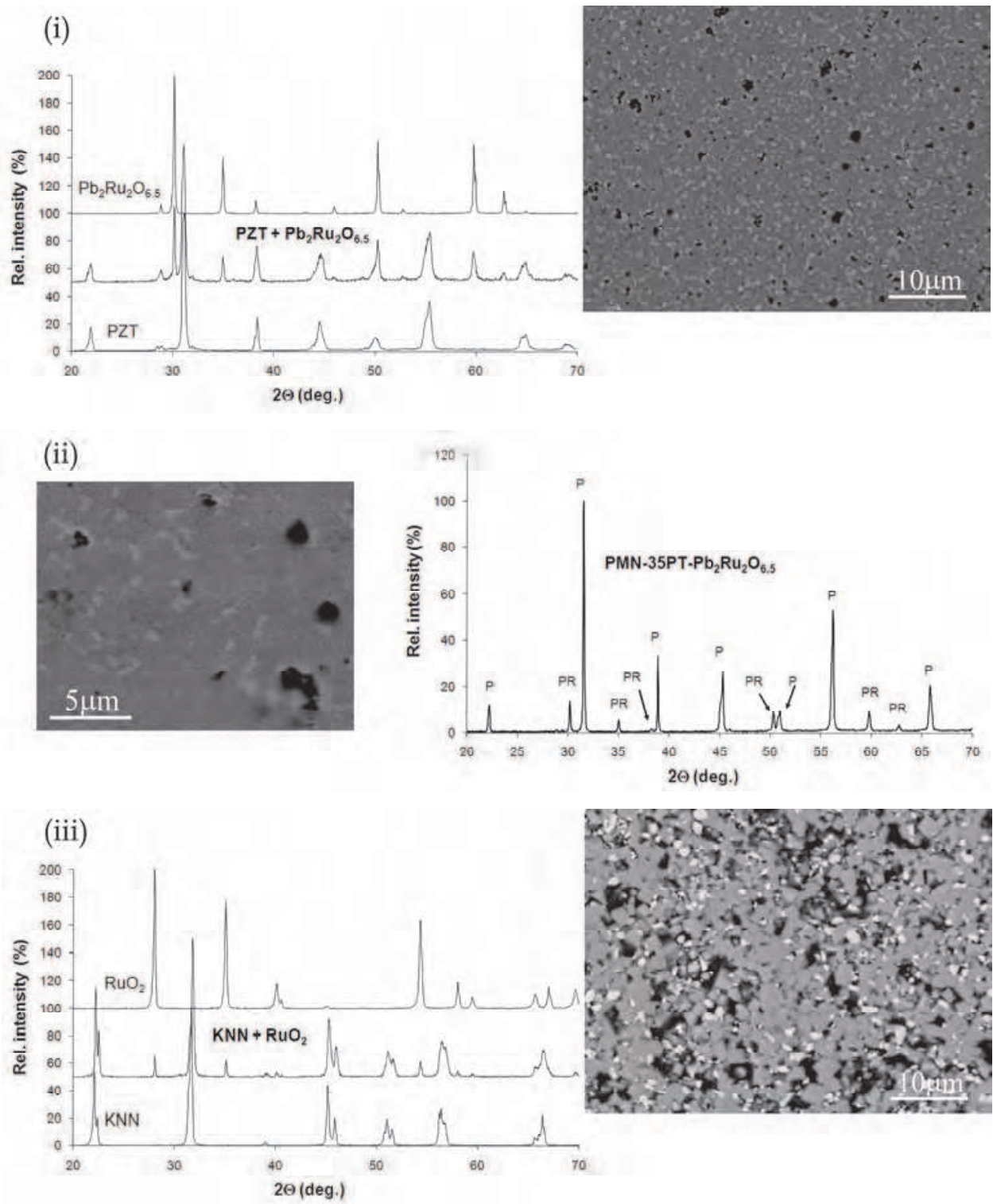
Fig. 3. Microstructures and X-ray spectra of developed all-ceramic percolative composites: (i) PZT–$Pb_2Ru_2O_{6.5}$ with 15 vol. % of $Pb_2Ru_2O_{6.5}$; (ii) PMN-35PT–$Pb_2Ru_2O_{6.5}$ with 15 vol. % of $Pb_2Ru_2O_{6.5}$; (iii) KNN–RuO_2 with 15 vol. % of RuO_2. For comparison, the X-ray spectra of individual PZT, KNN, and $Pb_2Ru_2O_{6.5}$ constituents are included in (i) and (iii), while in the PMN-35PT–$Pb_2Ru_2O_{6.5}$ X-ray spectrum peaks of the PMN-35PT and $Pb_2Ru_2O_{6.5}$ are denoted with P and PR, respectively.

4. Dielectric response of composites

Samples of 5–6 mm in diameter with sputtered gold electrodes on both surfaces were used for dielectric characterization. The complex dielectric constant $\varepsilon^*(\nu,T)=\varepsilon'-i\varepsilon''$ was measured as a function of the frequency (ν; 20 Hz to 1 MHz) and temperature (T; heating and cooling rates of $\pm 0.5°Cmin^{-1}$) using an HP4284A precision LCR meter. The amplitude of the probing ac electric signal, applied to samples with a thickness of $\approx$300 μm, was 1 V. The temperature was stabilized using a lock-in bridge technique with a Pt100 resistor as a thermometer. The real part of the complex ac-conductivity $\sigma^*(\nu,T)=\sigma'+i\sigma''$ was calculated via $\sigma'=2\pi\nu\varepsilon_0\varepsilon''$ with ε_0 being the permittivity of free space.

4.1 Qualitative description of the frequency spectra

The frequency dependence of the room-temperature dielectric constant ε' and conductivity σ' in PZT–$Pb_2Ru_2O_{6.5}$ samples with different $Pb_2Ru_2O_{6.5}$ volume concentrations is shown in Fig. 4. There exist several mixing formulae, or even different approaches, which predict or describe the dielectric response of a two-component heterogeneous system. For example, a detected behavior of the electrical conductivity – at higher frequencies σ' increases, while at lower frequencies values tend toward the dc-conductivity plateau – could easily be modeled by an equivalent circuit composed of two RC circuits connected in serial. The resistivity of the low-frequency plateau is then R_1+R_2, while at higher frequencies the conductivity follows a ν^2 law if $R_2 \gg R_1$ (Efros & Shklovskii, 1976), as is, evidently, the case in a percolative composite (then the value of the low-frequency plateau is just the resistivity of the matrix). However, although a crossover from the plateau to the ν^2 dependence has in fact been observed in the $Al_6Si_2O_{13}$-molybdenum composite (Pecharroman & Moya, 2000), the $\sigma'(\nu)$ increase here is much weaker. This is not surprising, as for granular systems, rather than modeling the spectra by various equivalent circuits with frequency-independent elements, more physically transparent models are needed in order to adequately describe their effective dielectric response.

The complex electrical conductivity of different metal-insulator composites can often be described by the two exponent phenomenological percolation equation – an excellent review of this method is given in (Chiteme et al., 2007). The equation is also known as the general effective medium equation. In fact, by using the effective medium approach (EMA – assuming that the probing field is homogeneous within the individual particles) it has been derived that the ac conductivity in a random system follows a ν^s behavior with s<1 (Springett, 1973), as has in fact been detected in our composites. In the limit of EMA also a rather general approach has been formulated (Petzelt & Rychetsky, 2005), which states that for any two-component composite with sharp particle boundaries the dielectric response can be composed of two additive parts. One part describes the sum of the original bulk responses weighted by the relative volumes, while the second part describes the localized particles affected by the depolarization field depending on particle shape and its surroundings. Within this approach, the spherical shape of inclusions leads to a percolation threshold of 1/3 (Rychetsky et al., 1999), thus a more general particle form and topology would be needed to describe smaller threshold, as is frequently observed (also in our case, as will be shown in the next subsection). However, the detected dielectric response of all developed composites (see PZT–$Pb_2Ru_2O_{6.5}$ in Fig. 4, PMN-PT–$Pb_2Ru_2O_{6.5}$ in Fig. 5, and KNN-RuO_2 in Fig. 6) can be qualitatively understood:

At lower frequencies the conductivity of the $Pb_2Ru_2O_{6.5}$ or RuO_2 inclusions is effectively blocked, while at sufficiently high frequencies their higher conductivity is revealed since most of the charge carriers have no time to feel the blocking boundaries. The effective ac-conductivity σ' therefore increases with frequency (and would increase up to the high-frequency plateau corresponding to the value of the $Pb_2Ru_2O_{6.5}$ or RuO_2 conductivity). As even for an inhomogeneous system the Kramers-Kronig relations must be satisfied, the increasing σ' contribute to the static dielectric constant via a strong dielectric relaxation. In systems with the composition very close to the percolation threshold (the PZT–$Pb_2Ru_2O_{6.5}$ composite with 17 vol. % of $Pb_2Ru_2O_{6.5}$ in Fig. 4 and the lead-free KNN-RuO_2 composite with 20 vol. % of RuO_2 in Fig. 6), ac-conductivity is almost frequency-independent in the entire experimental range. Considering the Kramers-Kronig relations, we may conclude that here the strong conductivity dispersion shifts below 10 Hz, as, on the other hand, the dielectric constant in these samples strongly increases at lower frequencies.
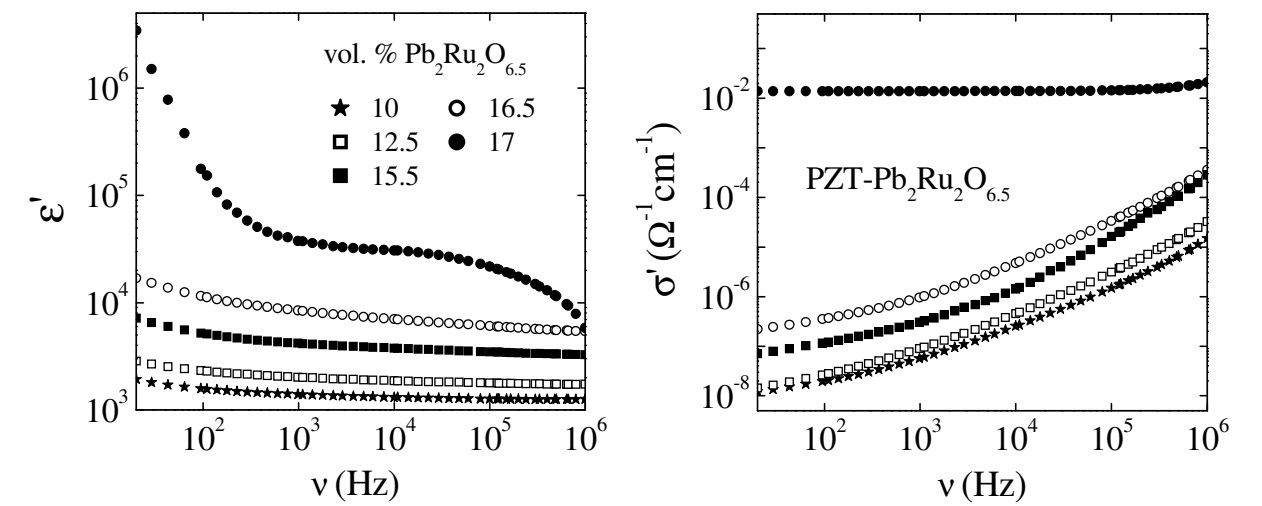

Fig. 4. Frequency dependence of the real parts of the complex dielectric constant ϵ' and conductivity σ' measured at room temperature for PZT–$Pb_2Ru_2O_{6.5}$ samples with different volume concentrations of $Pb_2Ru_2O_{6.5}$.
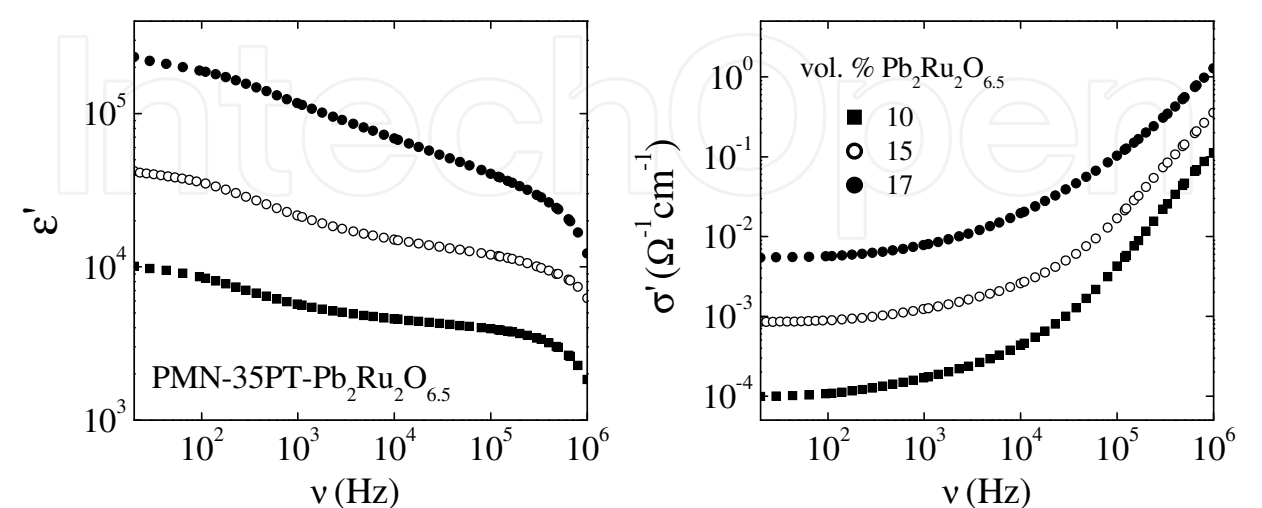

Fig. 5. Room-temperature dielectric constant and conductivity as a function of the frequency for PMN-35PT–$Pb_2Ru_2O_{6.5}$ samples with different $Pb_2Ru_2O_{6.5}$ volume concentrations.

In contrast to both lead-based systems, the experimental condition plays an important role in the KNN-RuO$_2$ composite, as being emphasized in Fig. 6. Here, the main frames show the frequency dependence of ε' and σ' in samples with different RuO$_2$ volume concentration, measured at room temperature under vacuum. While the evaluation of data on increasing RuO$_2$ content is very similar to that in the PZT–Pb$_2$Ru$_2$O$_{6.5}$ and PMN-35PT–Pb$_2$Ru$_2$O$_{6.5}$ systems, the low-pressure condition is very important. The inset namely clearly reveals that ε', measured in air, additionally strongly increases at lower frequencies. Most probably this is due to the conductivity contribution of water in the pores – in the KNN-RuO$_2$ these are much larger than in the lead-based composites (see Fig. 3). This is further endorsed by the fact that data taken under atmospheric pressure but with highly-hygroscopic silica-gel placed in the sample cell are almost identical to those detected under vacuum. Thus, all results, hereupon presented for the KNN-RuO$_2$ system, were obtained under vacuum, while the pressure condition did not play any role in denser lead-based PZT–Pb$_2$Ru$_2$O$_{6.5}$ and PMN-35PT–Pb$_2$Ru$_2$O$_{6.5}$ systems.
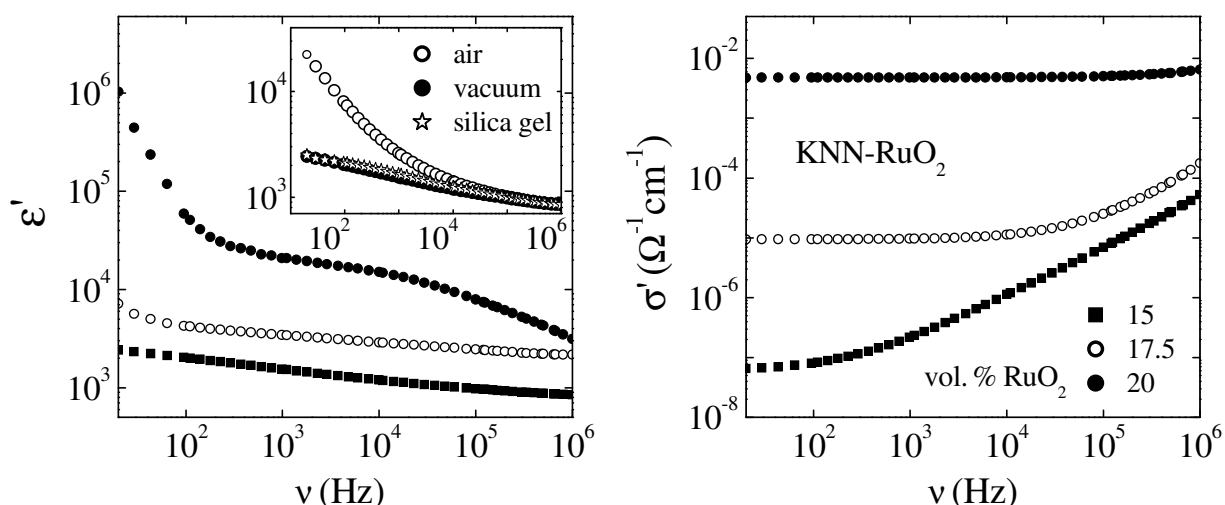

Fig. 6. Frequency dependence of ε' and σ' measured under vacuum at room temperature in KNN–RuO$_2$ samples with different volume concentrations of RuO$_2$. The inset shows data obtained in the sample with 15 vol. % of RuO$_2$ after three different treatment procedures.

4.2 Evolution of the dielectric constant vs. the conductive filler volume concentration

Values of the real part of the complex dielectric constant evidently strongly increase with higher conductive filler volume concentration (see ε'(ν) spectra for samples with different compositions in Figs. 4 to 6). This dependence is clearly depicted in Figs. 7 and 8, which show the evolution of ε' (measured at room temperature at the frequency of 1 kHz) in all developed all-ceramic percolative composites versus the conductive filler volume content. The solid line represents the fit of the experimental data to an expression derived from general percolation theories (Bergman & Imry, 1977; Efros & Shklovskii, 1976)

$$\varepsilon' = \varepsilon_m \left[(p_c - p)/p_c \right]^{-q}, \tag{3}$$

which has been, up to now, successfully applied to several organic and inorganic percolative composites (Huang et al., 2004; Pecharroman et al., 2001; Song et al., 1986). Here, ε$_m$ is the

real part of the complex dielectric constant of the insulator matrix, p is the volume concentration of the conductive admixture, p_c is the percolation threshold for the conduction (unambiguously defined in the ideal composite with the zero conductivity of the matrix via $\sigma_{dc}=0$ for $p<p_c$), and q is the critical exponent. Several values for the percolation critical exponents and the threshold value have been proposed on the basis of theoretical derivations (Bergman & Imry, 1977; Efros & Shklovskii, 1976; Feng et al., 1987) or numerical calculations (Straley, 1977; Webman et al., 1975). While standard percolation theories on three-dimensional lattices assume $q\approx0.9$ and $p_c\approx0.16$ (Kirkpatrick, 1973), rather different values (usually a much higher p_c) have been experimentally detected in various percolative systems, which can be explained in terms of the continuous percolation theory (Feng et al., 1987). Here, the fit of the PZT–$Pb_2Ru_2O_{6.5}$ data yields $q=0.723\pm0.004$ and $p_c=0.171\pm0.001$. It is interesting that almost identical value of q has been detected in the samples consisting of small Ag particles, randomly embedded in a non-conducting KCL host (Grannan et al., 1981) and also predicted by numerical calculations performed on a cubic lattice of resistors with two possible values of resistance (Straley, 1977). The fit of the KNN–RuO_2 data yields $q=1.05\pm0.04$ (q=1 is obtained in the framework of the effective medium approach regardless of the space dimensionality (Efros & Shklovskii, 1976)) and $p_c=0.205\pm0.004$, and the fit of the PMN-35PT–$Pb_2Ru_2O_{6.5}$ data yields $q=0.89\pm0.04$ and $p_c=0.174\pm0.003$. However, the most important fact is that exact fits of ε' in Figs. 7 and 8 further confirms the perfect outgrowth of the PZT–$Pb_2Ru_2O_{6.5}$, PMN-35PT–$Pb_2Ru_2O_{6.5}$, and KNN–RuO_2 composites, with the dielectric constant near the percolation threshold being for two orders of magnitude higher than in the pure matrix (PZT, PMN-35PT, or KNN) ferroelectric ceramics – this hold true also for the PMN-35PT–$Pb_2Ru_2O_{6.5}$ and KNN–RuO_2 composites, where a significant fraction of porosity, which can clearly be seen in Fig. 3 (and is many times observed in KNN-based ceramic composites (Sun et al., 2008)) undoubtedly alters the dielectric response, i.e., decreases the dielectric constant.
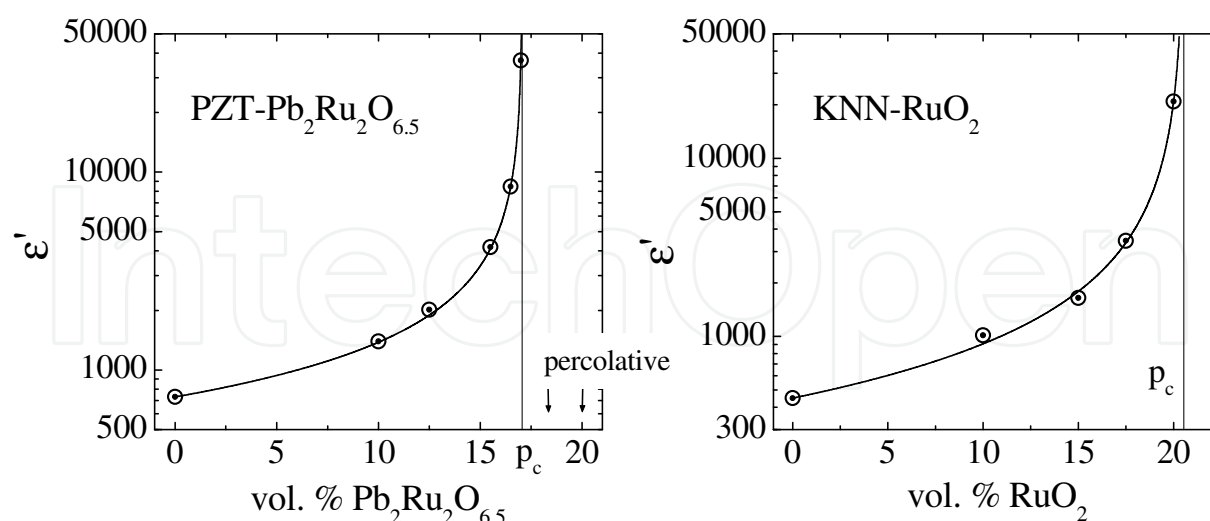

Fig. 7. The real part of the complex dielectric constant of the PZT–$Pb_2Ru_2O_{6.5}$ and KNN–RuO_2 composites vs. the conductive filler volume content, measured at room temperature at the frequency of 1 kHz. Solid lines represent fits of the experimental data to Eq. (3), while vertical lines indicate the percolation threshold p_c. Arrows indicate two percolative, i.e., electrically conductive PZT–$Pb_2Ru_2O_{6.5}$ samples – their ε' values cannot be determined.

It should once again be stressed out that the effective conductivity, similar as the effective dielectric constant (Eq. (3)), exhibits a critical behavior in the vicinity of p_c (see Eqs. (1) and (2)), while at the percolation point σ' undergoes an abrupt discontinuity. Such a behavior is clearly depicted in Fig. 8 for the PMN-35PT–$Pb_2Ru_2O_{6.5}$ system. Consequently, the dielectric loss factor $\tan\delta = \varepsilon''/\varepsilon'$ becomes extremely high near p_c (see Fig. 9). Thus, percolative samples with compositions near the percolation threshold are by default not suitable for applications where the dielectric loss factor should be small. However, the electrical conductivity in samples with lower conductive filler concentration, where dielectric constant is still much
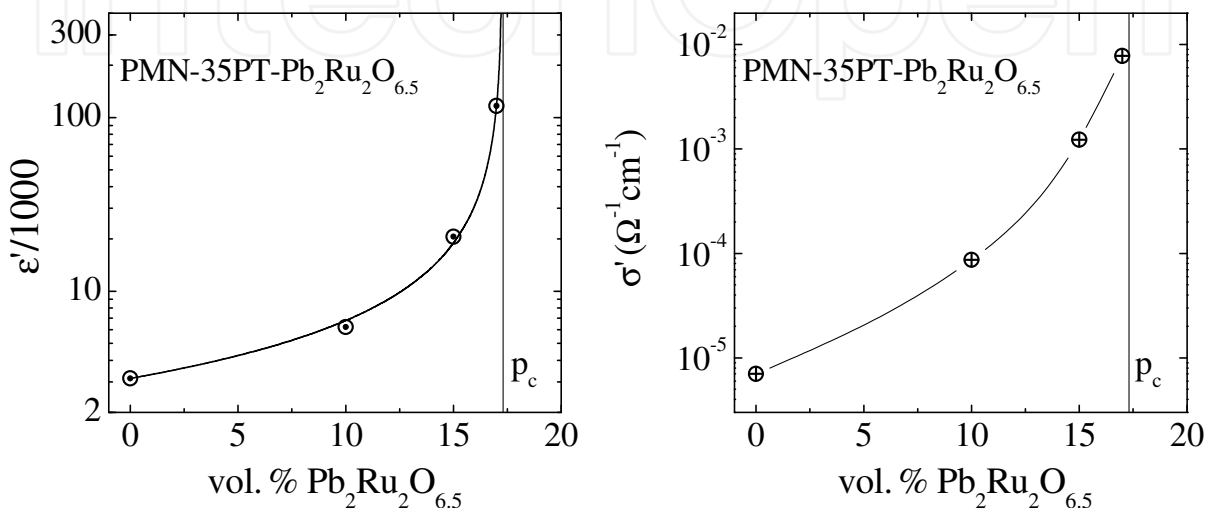

Fig. 8. Evolution of the dielectric constant and the dependence of the electrical conductivity on the $Pb_2Ru_2O_{6.5}$ volume content in PMN-35PT–$Pb_2Ru_2O_{6.5}$ samples at room temperature at the frequency of 1 kHz. The solid line through the ε' experimental data is the fit to Eq. (3). The solid line through the σ' data is a guide to the eye, while vertical lines in both graphs denote the percolation threshold.
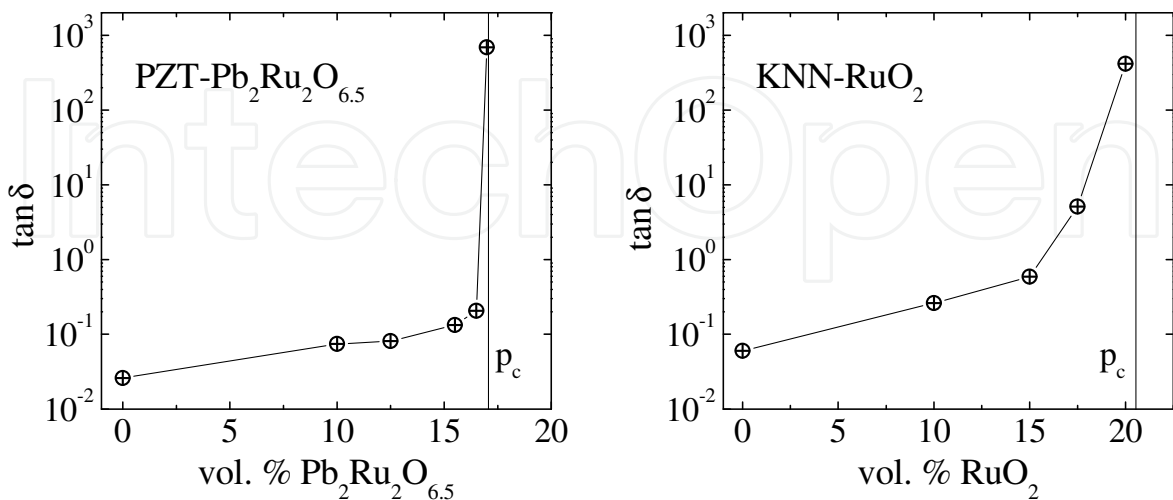

Fig. 9. Dependence of the dielectric loss factor $\tan\delta = \varepsilon''/\varepsilon'$ on the conductive filler volume concentration in the PZT–$Pb_2Ru_2O_{6.5}$ and KNN–RuO_2 all-ceramic percolative composites. Solid lines are guides to the eye.

higher than in the pure matrix ceramic system, are supposedly acceptable for applications – for example, PZT–$Pb_2Ru_2O_{6.5}$ samples with p<0.165 (see Figs. 7 and 9), where $tan\delta$<0.1, while dielectric constant still reaches values above 5000.

4.3 Temperature stability of the response

The temperature dependence of the dielectric constant ε' and ac electrical conductivity σ', measured at various frequencies in the PZT–$Pb_2Ru_2O_{6.5}$ sample (10 vol. % of $Pb_2Ru_2O_{6.5}$), is shown in Fig. 10 for the temperature interval of -125°C–125°C. Although above room temperature, due to the increasing conductivity, ε' at lower frequencies strongly increases, the detected dependences are rather smooth around room temperature. Similar conclusion applies for the KNN–RuO_2 system – $\varepsilon'(T)$ detected at two frequencies in the sample with 15 vol. % of RuO_2 is shown in the inset to Fig. 10.
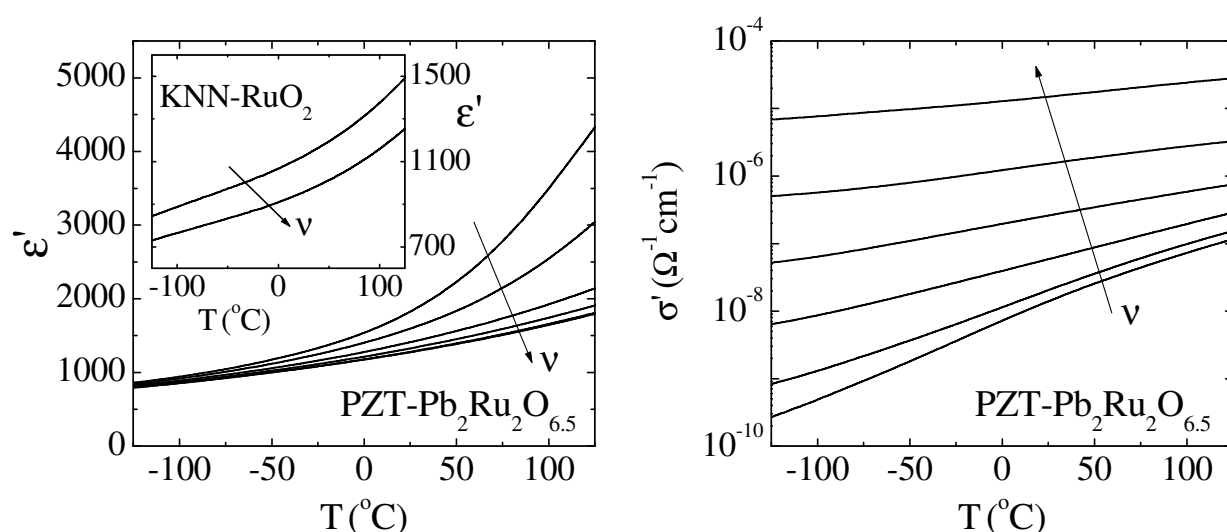

Fig. 10. Temperature dependence of the dielectric constant and ac electrical conductivity, measured at several frequencies (30 Hz, 100 Hz, 1 kHz, 10 kHz, 100 kHz, 1 MHz, order indicated by arrows) in the PZT–$Pb_2Ru_2O_{6.5}$ sample with 10 vol. % of $Pb_2Ru_2O_{6.5}$. The inset shows ε' measured as a function of the temperature at two frequencies (100 kHz, 1 MHz) in the KNN–RuO_2 sample with 15 vol. % of RuO_2.

While temperatures of the paraelectric-to-ferroelectric phase transition in the PZT and KNN systems are much above the highest measured temperature (≈370°C in the PZT and ≈420°C in the KNN), this phase transition, taking place in the matrix, dominates the temperature dependence of the PMN-35PT–$Pb_2Ru_2O_{6.5}$ composite in the measured temperature range. Fig. 11 shows the temperature dependence of the dielectric constant and ac electrical conductivity, detected at various frequencies in the PMN-35PT–$Pb_2Ru_2O_{6.5}$ sample with 15 vol. % of $Pb_2Ru_2O_{6.5}$. The paraelectric-to-ferroelectric phase transition in the pure PMN-PT system of this composition takes place at T_c≈165°C (Colla et al., 1998), but, as can be seen in Fig. 11, becomes slightly diffusive in a heterogeneous composite system – the $\varepsilon'(T)$ and $\sigma'(T)$ maxima are frequency dependent here and at temperatures lower than T_c. We may, however, as in the case of PZT–$Pb_2Ru_2O_{6.5}$ and KNN–RuO_2 systems, still conclude that at higher frequencies the temperature dependence is relatively smooth in the range around room temperature, i.e., in the temperature range most interesting for eventual applications.
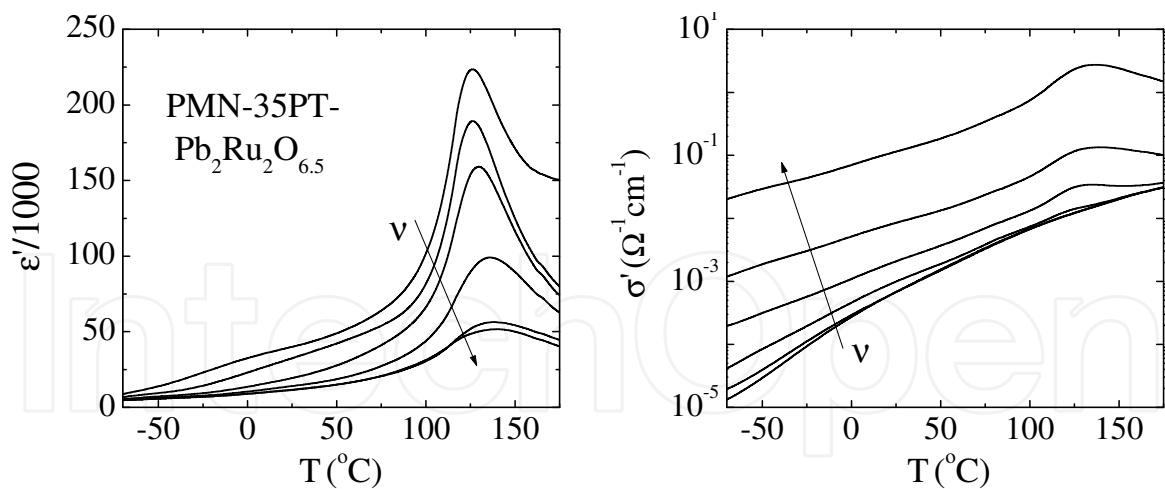
Fig. 11. Temperature dependence of the dielectric constant and ac electrical conductivity, detected at various frequencies (20 Hz, 100 Hz, 1 kHz, 10 kHz, 100 kHz, 1 MHz, order indicated by arrows) in the PMN-35PT–Pb$_2$Ru$_2$O$_{6.5}$ sample with 15 vol. % of Pb$_2$Ru$_2$O$_{6.5}$.

4.4 Feasibility of electric-field poling

As stated in the introduction, high dielectric constant materials are highly desirable for use not only as capacitor dielectrics but also in a broad range of advanced electromechanical applications, where mainly their piezoelectric response is employed.

The piezoelectric effect is the linear electromechanical interaction between the mechanical and the electrical state in crystalline materials with no inversion symmetry. It is a reversible process: materials that exhibit the direct piezoelectric effect – the internal generation of electrical charge resulting from an applied mechanical force, also exhibit the reverse effect – the internal generation of a mechanical force resulting from an applied electrical field.

The electrical and mechanical behavior of the material is generally described by the strain-charge coupled equations:

$$\{S\}=[s^E]\{T\}+[d^t]\{E\}, \tag{4}$$

$$\{D\}=[d]\{T\}+[\varepsilon^T]\{E\}. \tag{5}$$

Here, {S} and {T} are strain and stress vectors, respectively, while {D} and {E} represent vectors of the electric displacement and electric field. [ε] and [s] are dielectric constant and compliance tensors, while [d] is the direct piezoelectric effect tensor and [d^t] is the converse piezoelectric effect tensor. The superscript E indicates a zero or constant electric field, the superscript T indicates a zero or constant stress field, and the superscript t stands for transposition of a matrix.

For a material of the 4mm – case of poled tetragonal piezoelectric ceramics (Jaffe et al., 1971) – and of the 6mm crystal class, Eqs. (4) and (5) simplify in the case of zero stress field into

$$\begin{bmatrix} S_1 \\ S_2 \\ S_3 \\ S_4 \\ S_5 \\ S_6 \end{bmatrix} = \begin{bmatrix} 0 & 0 & d_{31} \\ 0 & 0 & d_{32} \\ 0 & 0 & d_{33} \\ 0 & d_{24} & 0 \\ d_{15} & 0 & 0 \\ 0 & 0 & 0 \end{bmatrix} \begin{bmatrix} E_1 \\ E_2 \\ E_3 \end{bmatrix} \; ; \; \begin{bmatrix} D_1 \\ D_2 \\ D_3 \end{bmatrix} = \begin{bmatrix} \varepsilon_{11} & 0 & 0 \\ 0 & \varepsilon_{22} & 0 \\ 0 & 0 & \varepsilon_{33} \end{bmatrix} \begin{bmatrix} E_1 \\ E_2 \\ E_3 \end{bmatrix} \tag{6}$$

using the Nye notation, in which elastic constants and elastic moduli are labeled by replacing the pairs of letters xx, yy, zz, yz, zx, and xy by the number 1, 2, 3, 4, 5, and 6, respectively. This means that the external electric field generates electric displacement, i.e., electric polarization, and strain through the converse piezoelectric effect.

However, ceramic materials are multicrystalline structures made up of large numbers of randomly orientated crystal grains. The random orientation of the grains results in a net cancelation of the piezoelectric effect. Thus, the ceramic material must be poled – a dc bias electric field is applied (usually the fired ceramic piece is cooled through the Curie point under the influence of the field) which aligns the ferroelectric domains, resulting in a net piezoelectric effect.

As the electrical conductivity of percolative composites strongly increases on approaching the percolation threshold, the feasibility of poling the PZT- $Pb_2Ru_2O_{6.5}$ samples has been checked. PZT- $Pb_2Ru_2O_{6.5}$ system has been chosen as its electrical conductivity is much lower than in the PMN-35PT–$Pb_2Ru_2O_{6.5}$ system or in the KNN–RuO_2 samples which are not treated under vacuum. After poling the PZT-$Pb_2Ru_2O_{6.5}$ samples with a high dc bias electric field, the piezoelectric coefficient d_{33} (strain in the direction of the applied measuring field) has been measured using a small ac voltage. It should be noted that, while various piezoelectric coefficients are usually determined and thus the indication is absolutely necessary, the dielectric constant is almost without exception determined in the direction of the applied field, i.e., ε' without indices in fact denotes the dielectric constant ε_{33}.

Results of piezoelectric characterization are shown in Fig. 12. While in samples, which are very close to the percolation threshold, the breakdown electric field is below 5 kV/cm, samples with lower $Pb_2Ru_2O_{6.5}$ content can be poled with the dc bias electric fields higher than 30 kV/cm. It is thus once again revealed that percolative samples with compositions near the percolation threshold are not very suitable for applications, while samples with lower conductive filler concentration, where dielectric constant is still much higher than in the pure ceramic matrix, are very promising for use as high dielectric constant materials.
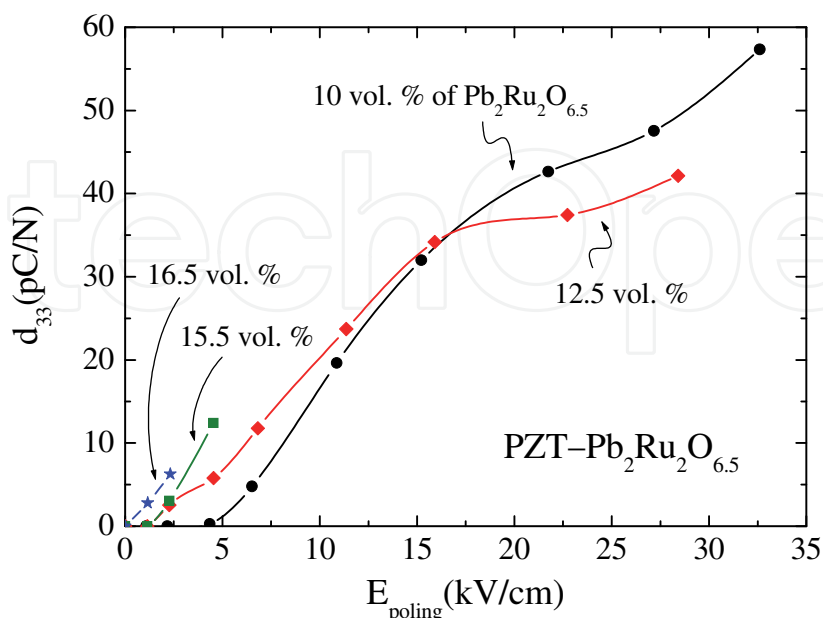

Fig. 12. Piezoelectric coefficient d_{33} in various PZT-$Pb_2Ru_2O_{6.5}$ samples, measured with small ac voltage, after poling the sample with a high dc bias electric field (E_{poling}).

5. Conclusion

Development of all-ceramic percolative composites
i.   PZT-$Pb_2Ru_2O_{6.5}$
ii. PMN-35PT–$Pb_2Ru_2O_{6.5}$ and
iii. KNN–RuO_2

based on the perovskite ferroelectric and ruthenium-based conductive ceramics is reported in this chapter. The structural analysis revealed that there were no chemical reactions between the constituents during processing, which resulted in a perfect structure of composites – conductive ceramic grains are uniformly distributed throughout the ferroelectric ceramic matrix. Thus, in the lead-based PZT-$Pb_2Ru_2O_{6.5}$ and PMN-35PT–$Pb_2Ru_2O_{6.5}$ and in the lead-free KNN–RuO_2 systems the dielectric response in fact follows the predictions of the percolation theory. As a result, the dielectric constant strongly increases on the conductive filler increasing content, reaching values near the percolation threshold that are for two orders of magnitude higher than in the pure matrix ceramics. Furthermore, the determined critical exponents and percolation points agree reasonably with the theoretically predicted values. The frequency- and temperature-dependent dielectric response of all developed systems is also presented and discussed.

Finally, not only structural and dielectric results, i.e., a successful synthesis of lead-based and lead-free percolative systems exhibiting a stable giant dielectric response, but also electromechanical properties demonstrate the potential of all-ceramic percolative composites for use as high-dielectric-constant materials in various applications.

6. Acknowledgment

7. References

Bergman, D. J. & Imry, Y. (1977). Critical behavior of the complex dielectric constant near the percolation threshold of a heterogeneous material. *Physical Review Letters*, Vol. 39, Iss. 19, Nov. 1977, pp. 1222-1225, ISSN 0031-9007.

Bobnar, V.; Hrovat, M.; Holc, J. & Kosec, M. (2008). Giant dielectric response in Pb(Zr,Ti)O$_3$–$Pb_2Ru_2O_{6.5}$ all-ceramic percolative composite. *Applied Physics Letters*, Vol. 92, Iss. 18, May 2008, 182911 3pp., ISSN 0003-6951.

Bobnar, V.; Hrovat, M.; Holc, J.; Filipič, C.; Levstik, A. & Kosec, M. (2009a). Colossal dielectric response in all-ceramic percolative composite 0.65Pb(Mg$_{1/3}$Nb$_{2/3}$)O$_3$-0.35PbTiO$_3$-$Pb_2Ru_2O_{6.5}$. *Journal of Applied Physics*, Vol. 105, Iss. 3, Feb. 2009, 034108 5pp., ISSN 0021-8979.

Bobnar, V.; Hrovat, M.; Holc, J. & Kosec, M. (2009b). All-ceramic lead-free percolative composite with a colossal dielectric response. *Journal of the European Ceramic Society*, Vol. 29, Iss. 4, Mar. 2009, pp. 725-729, ISSN 0955-2219.

Chiteme, C.; McLachlan, D. S. & Sauti, G. (2007). ac and dc percolative conductivity of magnetite-cellulose acetate composites. *Physical Review B*, Vol. 75, Iss. 9, Mar. 2007, 094202 13pp., ISSN 1098-0121.

Colla, E. V.; Yushin, N. K. & Viehland, D. (1998). Dielectric properties of $(PMN)_{(1-x)}(PT)_x$ single crystals for various electrical and thermal histories. *Journal of Applied Physics*, Vol. 83, Iss. 6, Mar. 1998, pp. 3298-3304, ISSN 0021-8979.

Dang, Z.-M.; Lin, Y.-H. & Nan, C.-W. (2003). Novel ferroelectric polymer composites with high dielectric constants. *Advanced Materials*, Vol. 15, Iss. 19, Oct. 2003, pp. 1625-1629, ISSN 0935-9648.

Deepa, K. S.; Sebastian, M. T. & James, J. (2007). Effect of interparticle distance and interfacial area on the properties of insulator-conductor composites. *Applied Physics Letters*, Vol. 91, Iss. 20, Nov. 2007, 202904 3pp., ISSN 0003-6951.

Efros, A. L. & Shklovskii, B. I. (1976). Critical behaviour of conductivity and dielectric constant near the metal-non-metal transition threshold. *Physica Status Solidi (b)*, Vol. 76, Iss. 2, Aug. 1976, pp. 475-485, ISSN 0370-1972.

Feng, S.; Halperin, B. I. & Sen, P. N. (1987). Transport properties of continuum systems near the percolation threshold. *Physical Review B*, Vol. 35, Iss. 1, Jan. 1987, pp. 197-214, ISSN 1098-0121.

Grannan, D. M.; Garland, J. C. & Tanner, D. B. (1981). Critical behavior of the dielectric constant of a random composite near the percolation threshold. *Physical Review Letters*, Vol. 46, Iss. 5, Feb. 1981, pp. 375-378, ISSN 0031-9007.

Hrovat, M.; Benčan, A.; Holc, J. & Kosec, M. (2001). Subsolidus phase equilibria in the RuO_2–TiO_2–ZrO_2 system. *Journal of Materials Science Letters*, Vol. 20, Iss. 22, Nov. 2001, pp. 2005-2008, ISSN 0261-8028.

Huang, C. & Zhang, Q. M. (2004). Enhanced dielectric and electromechanical responses in high dielectric constant all-polymer percolative composites. *Advanced Functional Materials*, Vol. 14, Iss. 5, May 2004, pp. 501-506, ISSN 1616-301X.

Huang, C.; Zhang, Q. M.; deBotton, G. & Bhattacharya, K. (2004) All-organic dielectric-percolative three-component composite materials with high electromechanical response. *Applied Physics Letters*, Vol. 84, Iss. 22, May 2004, pp. 4391-4393, ISSN 0003-6951.

Jaffe, B.; Cook, W. R. & Jaffe, H. (1971). *Piezoelectric Ceramics,* Academic Press, New York, ISBN 0-12-379550-89.

Kirkpatrick, S. (1973). Percolation and conduction. *Reviews of Modern Physics*, Vol. 45, Iss. 4, Oct. 1973, pp. 574-588, ISSN 0034-6861.

Kuščer, D.; Holc, J.; Kosec, M. & Meden, A. (2006). Mechano-synthesis of lead–magnesium–niobate ceramics. *Journal of the American Ceramic Society*, Vol. 89, Iss. 10, Oct. 2006, pp. 3081-3088, ISSN 1551-2916.

Kuščer, D.; Holc, J. & Kosec, M. (2007). Formation of $0.65Pb(Mg_{1/3}Nb_{2/3})O_3$–$0.35PbTiO_3$ using a high-energy milling process. *Journal of the American Ceramic Society*, Vol. 90, Iss. 1, Jan. 2007, pp. 29-35, ISSN 1551-2916.

Li, J.-F.; Takagi, K.; Terakubo, N. & Watanabe, R. (2001). Electrical and mechanical properties of piezoelectric ceramic/metal composites in the $Pb(Zr,Ti)O_3/Pt$ system. *Applied Physics Letters*, Vol. 79, Iss. 15, Oct. 2001, pp. 2441-2443, ISSN 0003-6951.

Pecharroman, C. & Moya, J. S. (2000). Experimental evidence of a giant capacitance in insulator-conductor composites at the percolation threshold. *Advanced Materials*, Vol. 12, Iss. 4, Feb. 2000, pp. 294-297, ISSN 0935-9648.

Pecharroman, C.; Esteban-Betegon, F.; Bartolome, J. F.; Lopez-Esteban, S. & Moya, J. S. (2001). New percolative BaTiO$_3$-Ni composites with a high and frequency-independent dielectric constant ($\varepsilon_r \approx 80000$). *Advanced Materials*, Vol. 13, Iss. 20, Oct. 2001, pp. 1541-1544, ISSN 0935-9648.

Petzelt, J. & Rychetsky, I. (2005). Effective dielectric function in high-permittivity ceramics and films. *Ferroelectrics*, Vol. 316, 2005, pp. 89-95, ISSN 0015-0193.

Pierce, J. W.; Kuty, D. W. & Larry, J. L. (1982). The chemistry and stability of ruthenium-based resistors. *Solid State Technology*, Vol. 25, Iss. 10, Oct. 1982, pp. 85-93, ISSN 0038-1101.

Priya, S.; Viehland, D. & Uchino, K. (2002). Importance of structural irregularity on dielectric loss in (1–x)Pb(Mg$_{1/3}$Nb$_{2/3}$)O$_3$–(x)PbTiO$_3$ crystals. *Applied Physics Letters*, Vol. 80, Iss. 22, Jun. 2002, pp. 4217-4219, ISSN 0003-6951.

Raymond, M. V. & Smyth, D. M. (1996). Defects and charge transport in perovskite ferroelectrics. *Journal of Physics and Chemistry of Solids*, Vol. 57, Iss. 10, Oct. 1996, pp. 1507-1511, ISSN 0022-3697.

Reynolds, T. G. III & Buchanan, R. C. (2004). Ceramic capacitor materials. In: *Ceramic Materials for Electronics*, Editor Buchanan, R. C., pp. 141-206, Marcel Dekker, ISBN 0-8247-4028-9, New York.

Rychetsky, I.; Hudak, O. & Petzelt, J. (1999). Dielectric properties of microcomposite ferroelectrics. *Phase Transitions*, Vol. 67, Iss. 4, 1999, pp. 725-739, ISSN 0141-1594.

Scott, J. F. (2007). Applications of modern ferroelectrics. *Science*, Vol. 315, Iss. 5814, Feb. 2007, pp. 954-959, ISSN 0036-8075.

Song, Y.; Noh, T. W.; Lee, S.-I. & Gaines, J. R. (1986). Experimental study of the three-dimensional ac conductivity and dielectric constant of a conductor-insulator composite near the percolation threshold. *Physical Review B*, Vol. 33, Iss. 2, Jan. 1986, pp. 904-908, ISSN 1098-0121.

Springett, B. E. (1973). Effective-medium theory for the ac behavior of a random system. *Physical Review Letters*, Vol. 31, No. 24, Dec. 1973, pp. 1463-1465, ISSN 0031-9007.

Straley, J. P. (1977). Critical exponents for the conductivity of random resistor lattices. *Physical Review B*, Vol. 15, Iss. 12, Jun. 1977, pp. 5733-5737, ISSN 1098-0121.

Sun, X.; Chen, J.; Yu, R.; Xing, X.; Qiao, L. & Liu, G. (2008). BiFeO$_3$-doped (Na$_{0.5}$K$_{0.5}$)NbO$_3$ lead-free piezoelectric ceramics. *Science and Technology of Advanced Materials*. Vol. 9, Iss. 2, Jun. 2008, 025004 4 pp., ISSN 1468-6996.

Takeshima, Y.; Shiratsuyu, K.; Takagi, H. & Sakabe, H. Y. (1997). Preparation and dielectric properties of the multilayer capacitor with (Ba,Sr)TiO$_3$ thin layers by metalorganic chemical vapour deposition. *Japanese Journal of Applied Physics*, Vol. 36, No. 9B, Sep. 1997, pp. 5870-5873, ISSN 0021-4922.

van Loan, P. R. (1972). Conductive ternary oxides of ruthenium, and their use in thick film resistor glazes. *American Ceramic Society Bulletin*, Vol. 51, No. 3, Mar. 1972, pp. 231-233, ISSN 0002-7812.

Webman, I.; Jortner, J. & Cohen, M. H. (1975). Numerical simulation of electrical conductivity in microscopically inhomogeneous materials. *Physical Review B*, Vol. 11, Iss. 8, Apr. 1975, pp. 2885-2892, ISSN 1098-0121.

Xu, J. & Wong, C. P. (2005). Low-loss percolative dielectric composite. *Applied Physics Letters*, Vol. 87, Iss. 8, Aug. 2005, 082907 3pp., ISSN 0003-6951.

Yoshida, K. (1990). Percolative conduction in a composite system of metal and ceramics. *Journal of the Physical Society of Japan*, Vol. 59, No. 11, Nov. 1990, pp. 4087-4095, ISSN 0031-9015.

Zhang, Q. M.; Li, H.; Poh, M.; Xia, F.; Cheng, Z.-Y.; Xu, H. & Huang, C. (2002). An all-organic composite actuator material with a high dielectric constant. *Nature*, Vol. 419, Issue 6904, Sep. 2002, pp. 284-287, ISSN 0028-0836.
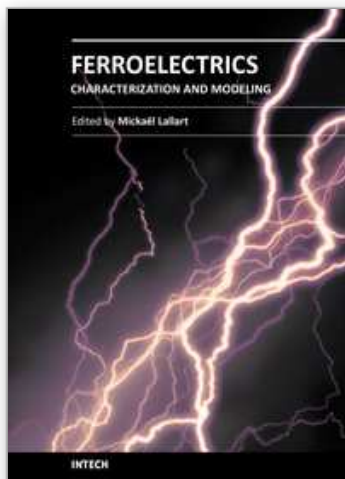
Ferroelectrics - Characterization and Modeling
Edited by Dr. Mickaël Lallart

Ferroelectric materials have been and still are widely used in many applications, that have moved from sonar towards breakthrough technologies such as memories or optical devices. This book is a part of a four volume collection (covering material aspects, physical effects, characterization and modeling, and applications) and focuses on the characterization of ferroelectric materials, including structural, electrical and multiphysic aspects, as well as innovative techniques for modeling and predicting the performance of these devices using phenomenological approaches and nonlinear methods. Hence, the aim of this book is to provide an up-to-date review of recent scientific findings and recent advances in the field of ferroelectric system characterization and modeling, allowing a deep understanding of ferroelectricity.

INTECH
open science | open minds